Optical and Quantum Electronics (2023) 55:652
https://doi.org/10.1007/s11082-023-04881-y

Broadband polarization insensitive metamaterial absorber

Ahmed S. Saadeldin[1] · Amr M. Sayed[1] · Adnan M. Amr[1] · Menna O. Sayed[1] · Mohamed Farhat O. Hameed[2,3,4] · S. S. A. Obayya[2,5]

Received: 30 January 2023 / Accepted: 25 April 2023 / Published online: 23 May 2023

Abstract
Ultrathin and broadband metamaterial absorber with loaded four lumped resistors is proposed and analyzed. The reported design is based on increasing the absorptivity by reducing the reflection and transmission coefficients simultaneously. Therefore, continuous metallic ground is used to achieve zero transmission while the reflection is reduced by matching the impedance of the proposed metamaterial absorber with the impedance of free space ($Z=Z_0$ or $\mu_r=\varepsilon_r$). Additionally, electric and magnetic resonances are achieved simultaneously with perfect absorptivity. The finite element method is used to simulate and analyze the reported absorber. The suggested absorber shows higher absorption than 90% over large frequency range (14.35–29.18 GHz) for both transverse electric and transverse magnetic polarizations. Further, the proposed design has high absorption through incident angle variation from 0° to 50°. Therefore, the reported perfect metamaterial absorber has good potential applications in communications, stealth and imaging fields.

Keywords Metamaterial · Perfect absorber · Plasmonics · Absorption

✉ Mohamed Farhat O. Hameed
mfarahat@zewailcity.edu.eg

✉ S. S. A. Obayya
sobayya@zewailcity.edu.eg

[1] Electronics and Communications Engineering Department, Akhbar Elyom Academy, 6th of October, Giza, Egypt

[2] Centre for Photonics and Smart Materials, Zewail City of Science, Technology and Innovation, October Gardens, 6th of October City, Giza 12578, Egypt

[3] Nanotechnology and Nanoelectronics Engineering Program, Zewail City of Science, Technology and Innovation, October Gardens, 6th of October City, Giza 12578, Egypt

[4] Mathematics and Engineering Physics Department, Faculty of Engineering, University of Mansoura, Mansoura 35516, Egypt

[5] Electronics and Communications Department, Faculty of Engineering, University of Mansoura, Mansoura 35516, Egypt

1 Introduction

Electromagnetic absorber has been attracted many researchers over few last decades due to their potential applications in civil and military applications such as Stealth Technology (Schurig et al. 2006), Specific Absorption Rate (SAR) Reduction (Fan et al. 2019), sensor applications (Saadeldin et al. 2019; Azab et al. 2021) and polarization control (Abouelatta et al. 2021a, b). Recently, metamaterial absorber has been introduced with high absorption over large bandwidth range. Metamaterial is engineered material to achieve properties not in nature ($\varepsilon < \varepsilon_0$ and $\mu < \mu_0$) (Engheta et al. 2006). So perfect metamaterial absorber attracts many interests for different applications. Perfect metamaterial is reported for first time by Landy (2008). The metamaterial absorber has advantages like compact size, lightweight and low profile. But it has a narrow bandwidth. In order to increase and enhance the narrow bandwidth, multilayer absorbers have been reported in Xiong et al. (2013), Cong et al. (2018) with thick structures. Further, multiple resonating structures (with different resonators or same resonators) in each unit cell can be used to overcome the narrow band problem (Fan et al. 2020). However, it is difficult to fit many different sizes of arrays in the same plane with inhomogeneous characteristics (Li et al. 2011). On the other hand, integrated the metamaterial absorber with lumped elements is another approach to enhance the narrow band limit (Nguyen et al. 2021). This approached has limit for using the lumped elements for THz ranges. But, for GHz range, the integration of lumped elements with metamaterial absorber is one of the most appropriate technique to obtain large enough bandwidth, high efficiency, and polarization insensitivity (Nguyen et al. 2021). In GHz range, perfect metamaterial absorbers have a relative larger size than that in the THz range where lumped elements can be integrated after the fabrication process (Watts et al. 2012). In Karaaslan et al. (2018), metamaterial absorber has been reported with multiple resonators of different sizes including lumped elements. The absorptivity of this design is between 80 to 99% through a frequency range of 3–5.9 GHz. Bağmancı et al. (2019) proposed a broadband metamaterial absorber based on split ring resonators which are loaded with lumped elements with absorptivity above 80% between 4 and 16 GHz. A broadband metamaterial absorber loaded with lumped resistors has been suggested with absorption above 90% over 7.12–8.61 GHz (Xiong et al. 2020). Chen et al. (2019) introduced a planar polarization-insensitive microwave metamaterial absorber loaded with lumped chip resistors with absorptivity above 90% from 8 to 18 GHz. Du et al. (2022) proposed ultra-thin low-frequency metamaterial absorber with lumped elements and magnetic material over frequency range from 1.24 to 3.14 GHz with absorption above 90%. Chen et al. (2021) demonstrated a wideband metamaterial absorber with lumped resistors over frequency range from 1.38 to 6.4 GHz. Recently, Suo et al. (2023) have investigated theoretically and experimentally a flexible transparent absorber with broadband absorption. A broadband absorber based on five layered structure was designed with four identical lumped resistors. An absorptivity above 90% was obtained over frequency range 14.3–28.3 GHz. Further, a perfect terahertz metamaterial absorber based on bulk Dirac semimetal and strontium titanate was numerically studied by Shen and Xiong (2022). The performance of the proposed design is flexibly controlled due to integrating two new materials with adjustable dielectric constant in one structure. The resonance frequency of the proposed absorber can be tuned from 0.67 to 0.72 THz by controlling the temperature of strontium titanate. While the absorptivity peak can be tuned by controlling the Fermi energy of bulk Dirac semimetal from 10 to 70 meV. Additionally, Wang and Cheng (2020), demonstrate experimentally a compact broadband metamaterial absorber based on meander wire structure with loaded a lumped resistors.

Such a design has absorptivity above 85% over frequency range from 1.84 to 5.96 GHz. Furthermore, a 3D circular periodic structure based on gypsum composite with carbon black was investigated as electromagnetic absorber by Xie et al. (2020). The reported design was suggested as a kind of green building materials that may be used to preventing health risks due to exposure of specific electromagnetic radiation. The absorber has absorption above 90% over frequency range from 2 to 8 GHz. Cheng et al. (2020) are proposed a broadband metamaterial absorber based on asymmetrical sectional resonators to improve the operating frequency band. The absorption over 90% is obtained over frequency range from 7.22 to 8.84 GHz. A 3D ultra-broadband tunable metamaterial absorber is presented by Zhang et al. (2021). The reported design is based on 3D glass cavity containing liquid metal and multi-layered structure. The tuned behavior can be controlled by the position of the liquid metal. The liquid metal poured into different position in the cavity due to rotating the structure. The absorption rate exceed 90% over 1.8–57.5 GHz for TE wave. While for TM wave, the absorption above 90% over 1.6–45.3 GHz. Xiong et al. (2022) demonstrate a broadband multilayered metamaterial absorber with optically transparent based on Indium Tin Oxide and polymethyl methacrylate. The absorption exceeds 90% over frequency range from 6.6 to 18 GHz. A dual-band terahertz perfect absorber based on InSb vertical-square-split-ring array structure is reported by Li et al. (2022). At room temperature of T = 295 K, the design has a dual-band perfect absorption with absorbance as high as 99.9% and 99.8% at 1.265 THz and 1.436 THz. Cheng et al. (2023) investigate theoretically a narrowband perfect metasurface absorber for sensing application in Terahertz region. The reported absorber is based on micro-ring array of GaAs backed with a gold ground-plane and dielectric substrate. The absorber has absorptivity of 99.9% at 2.213 THz. The suggested absorber shows a sensing performance with the sensitivity of 1.45 THz/RIU.

In this paper, an ultrathin, broadband and polarization insensitive loaded with four lumped resistors metamaterial absorber is numerically studied and analysed. The unit cell of the reported metamaterial absorber has a compact size (total area of 5.5 mm × 5.5 mm). The numerical analysis is carried out by using 3D full-wave simulator of the commercial computer simulation technology (CST) Microwave Studio software (http://www.cst.com). The suggested metamaterial absorber has absorptivity greater than 90% covering a broadband of frequencies (from 14.35 to 29.18 GHz). The achieved high absorptivity is due to the reduced reflection coefficient (through impedance matching) with zero transmission coefficient (by introducing metallic ground layer). Further, the proposed design has an ultrathin thickness of 0.076 λ at lowest frequency. Furthermore, the lumped resistors are used to increase the equivalent resistance to increase the absorption bandwidth. It is worth noting that most of the previously reported metamaterial absorber based on lumped elements with minimum unit cell dimensions of 10 × 10 × 3.25 mm with complex structures (Yoo et al. 2014; Ghosh et al. 2016; Chen et al. 2018; Kalraiya et al. 2019; Nguyen et al. 2018; Yang et al. 2007; Du et al. 2022; Chen et al. 2021). Therefore, the proposed design has advantages in terms of compactness, broadband, high absorption and polarization insensitivity with simple design.

2 Design considerations

Figure 1a, b show the unit cell of the proposed metamaterial absorber (MMA). The suggested MMA consists of top metallic layer with four surface mount resistor, dielectric substrate, and continuous metallic ground plane. The metallic layers is copper with a thickness

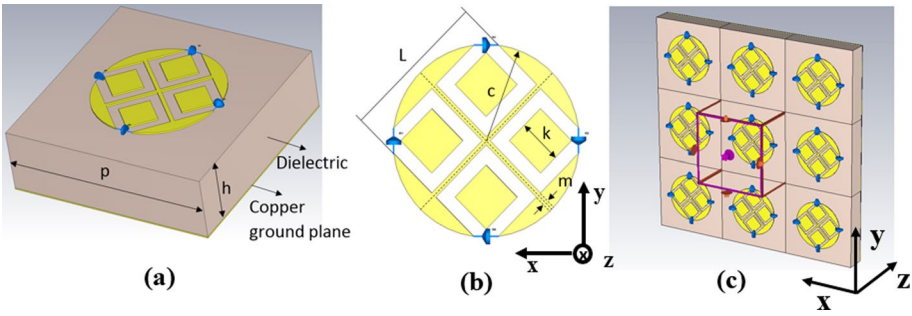

Fig. 1 The proposed metamaterial absorber **a** Isometric view of the unit cell, **b** Top view of the top metallic layer and **c** applied boundary conditions of the unit cell

of 0.035 mm and frequency independent conductivity $\sigma = 5.96 \times 10^7$ S/m. The dielectric substrate is made of low cost material FR-4 which has thickness (h) of 1.6 mm (0.076 λ at lowest frequency), relative dielectric constant of 4.3, and a loss tangent of 0.025 (Nguyen et al. 2021).

The 3D full-wave solver of the commercial computer simulation technology (CST) Microwave Studio software is used to analyse the suggested design. In this study, periodic boundary conditions are used around the unit cell in the x- and y-directions, while open boundary condition is set in the z-direction. Open boundary condition means that the simulator (CST) effectively places perfectly matched layer (operates like free space) as shown in Fig. 1c. The incident wave (plane wave) is propagating along z direction. The mesh of tetrahedral shape is utilized with an accuracy of 10^{-4}.

The metamaterial is artificial structured material with distinctive properties ($\varepsilon < \varepsilon_0$ and $\mu < \mu_0$) that cannot be realized in nature. The effective permittivity (ε_{eff}), effective permeability (μ_{eff}) and the relative impedance (Z_r) of the proposed MMA are calculated using the Eqs. (1), (2) and (3) (Nguyen et al. 2021). These parameters are obtained by inverting the calculated S-parameter to determine the impedance and hence, the values of the ε_{eff} and μ_{eff} can be obtained.

$$\varepsilon_{eff} = 1 + \frac{2j}{K_0 h}\left(\frac{1 - S_{11}}{1 + S_{11}}\right) \tag{1}$$

$$\mu_{eff} = 1 + \frac{2j}{K_0 h}\left(\frac{1 + S_{11}}{1 - S_{11}}\right) \tag{2}$$

$$Z_r = \sqrt{\frac{(1 + S_{11})^2 - S_{21}^2}{(1 - S_{11})^2 - S_{21}^2}} = \frac{1 + S_{11}}{1 - S_{11}} \tag{3}$$

where K_0 is the free space wavenumber, and h is the substrate thickness. Figure 2a, b shows the frequency dependent real and imaginary parts of both the effective permittivity and the effective permeability, respectively. Additionally, Fig. 2c represents the real and imaginary parts of the relative impedance. It may be seen from Fig. 2a, b that the value of the effective permittivity and effective permeability are equal through the operating band of frequencies. Also, it may be noted from Fig. 2c that the real part of the relative impedance

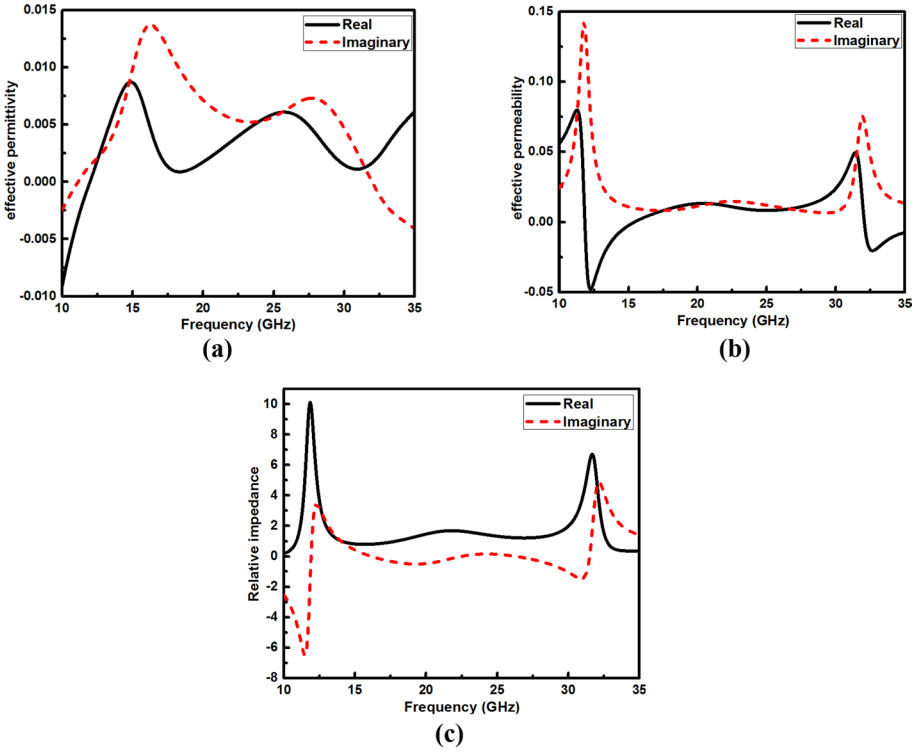

Fig. 2 The frequency dependent **a** effective permittivity, **b** effective permeability and **c** relative impedance of the suggested metamaterial absorber

is approximately unity through the absorption band. However, the imaginary part approximately equals to zero from 14 to 29 GHz.

3 Numerical results and discussion

The absorption coefficient (A) of the proposed MMA can be obtained through the reflectance (R) and transmittance (T) as shown in Eq. (4).

$$A = 1 - R - T = 1 - S_{11}^2 - S_{21}^2 \tag{4}$$

For the suggested design of MMA, the transmittance ($T = S_{21}^2$) is equal to zero due to the continuous metallic ground layer which behaves like perfect reflector. Consequently, the absorption coefficient can be determined through Eq. (5).

$$A = 1 - R = 1 - S_{11}^2 \tag{5}$$

Figure 3 shows the absorption of the reported MMA at normal incident for both transverse electric (TE) and transverse magnetic (TM) polarizations (red solid and blue dashed lines, respectively). In this investigation, the geometrical parameters are initially chosen as substrate thickness (h) = 1.6 mm, periodicity (p) = 5.5 mm, the radius of the metallic circle

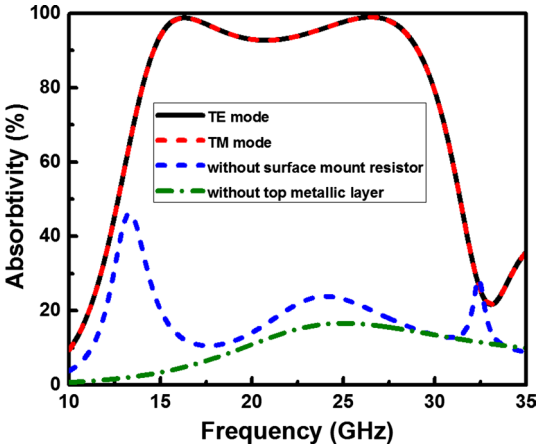

Fig. 3 The absorptivity of the suggested MMA at normal incident for TE, and TM modes, without top metallic layer and without surface mount resistors

in the top metallic layer (c) = 1.7 mm, the length of the etched square (L) = 2.7 mm, the length of the square patches (K) = 0.8 mm and the width of the metallic cross (m) = 0.1 mm. Additionally, the surface mount resistor is equal to 240 Ω. As shown in Fig. 3, the absorptivity is greater than 90% from 14.35 to 29.18 GHz. Also, the proposed MMA is insensitive to the polarization due to identical absorption response for both TE and TM polarizations. It may be seen from Fig. 3 (green dot-dashed line) that the absorption of the MMA without the top metallic layer (for TE mode) has a maximum absorptivity of 18% which indicates the impact of the top metallic layer on the absorption response. Further, the effect of the four surface mount resistors on the absorption response is investigated. Figure 3 (orange dashed line) shows the absorption of the proposed MMA without the lumped resistors (for TE mode). It is evident that the MMA without surface mount resistors becomes a dual band absorber rather than broadband absorber. So, the surface mount resistors have a direct impact on the impedance matching which affects the absorption of the suggested design.

In order to show the accuracy of our model, a comparative study is made with the simulated and measured absorptions of the metamaterial absorber reported by Cheng et al. (2020) shown in the inset of Fig. 4. It is evident from Fig. 4 that there is an excellent matching between our calculations based on FEM and that simulated in Cheng et al. (2020). Therefore, it is believed that our reported structure can be fabricated successfully. It is worth noting that the suggested geometrical parameters are in the same region of that fabricated in Cheng et al. (2020). Therefore, it is believed that the reported structure can be fabricated successfully.

In order to show the role of each element of the suggested design, the following structures shown in the inset of Fig. 5 are simulated. First, a metamaterial absorber with only top circular metallic patch is tested where dual band absorption is obtained at 16.18 GHz and 30.5 GHz with absorptivity of 19.87% and 82.38%, respectively. Then, a square shape is etched in the circular top metallic patch (design 2). The absorption performance shows three resonance peaks at 14.2 GHz, 25.78 GHz, and 30.94 GHz with absorptivity of 25.87%, 47.57%, and 97.5%, respectively. Next, design 3 is studied where three resonance peaks are supported at 15.43 GHz, 26.93 GHz, and 32.45 GHz with absorptivity of 21.48%, 68.16%, and 95.8%, respectively. Finally, the proposed design is suggested by loading four identical lumped resistors which achieves broad absorption band over frequency range 14.35–29.18 GHz with absorptivity above 90%.

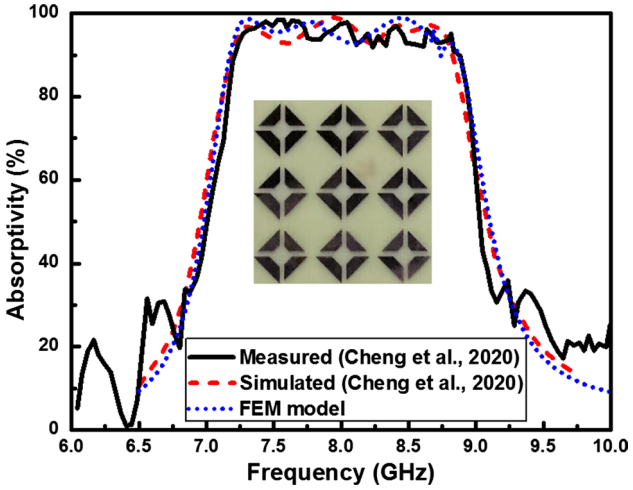

Fig. 4 Comparison between measured and calculated absorptivity with that obtained by the FEM model of the design reported by Cheng et al. (2020). The inset figure shows a schematic diagram of the fabricated design by Cheng et al. (2020)

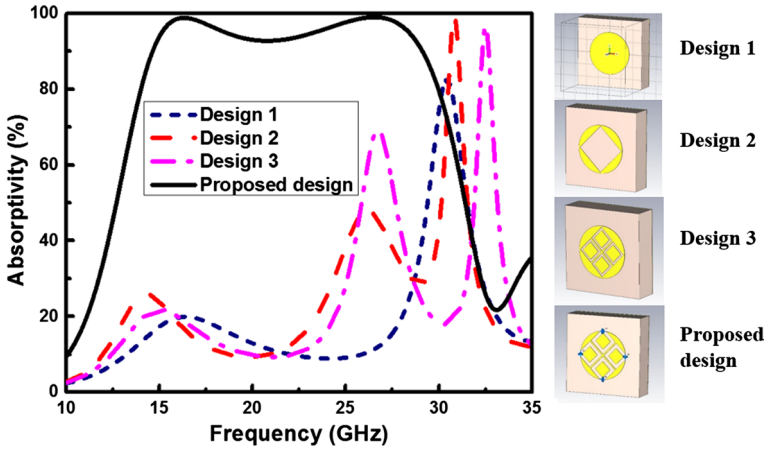

Fig. 5 Variation of the frequency dependent absorptivity of the studied four MMA designs

The impedance matching theory (Zhu 2018) can be used to explain the absorption mechanism. In this regard, perfect absorption can be obtained by making the reflection coefficient approximately equals to zero with zero transmission coefficient due to metallic ground plane. The reflection coefficient of the metamaterial absorber is given by (Landy 2008):

$$R_{TE} = \left| \frac{\mu_r cos\theta - \sqrt{n^2 - sin\theta}}{\mu_r cos\theta + \sqrt{n^2 - sin\theta}} \right|^2 \tag{6}$$

$$R_{TM} = \left| \frac{\varepsilon_r cos\theta - \sqrt{n^2 - sin\theta}}{\varepsilon_r cos\theta + \sqrt{n^2 - sin\theta}} \right|^2 \tag{7}$$

where θ is the incident angle and $n = \sqrt{\varepsilon_r \mu_r}$ is the effective refractive index of the metamaterial structure. For the normal incident $\theta = 0$, the reflection coefficient can be calculated by:

$$R = \left| \frac{Z - Z_0}{Z + Z_0} \right|^2 = \left| \frac{\sqrt{\mu_r} - \sqrt{\varepsilon_r}}{\sqrt{\mu_r} + \sqrt{\varepsilon_r}} \right|^2 \tag{8}$$

where Z is the impedance of the metamaterial absorber while Z_0 is the free space impedance.

$$A = 1 - R = 1 - \left| \frac{Z - Z_0}{Z + Z_0} \right|^2 = \left| \frac{\sqrt{\mu_r} - \sqrt{\varepsilon_r}}{\sqrt{\mu_r} + \sqrt{\varepsilon_r}} \right|^2 \tag{9}$$

It may be seen from Eq. (9) that perfect absorption can be obtained when the impedance matching ($Z = Z_0$ or $\mu_r = \varepsilon_r$) is achieved. In order to achieve the impedance matching, the presence of the electric and magnetic resonance simultaneously is required. The confirmation of this theory is obtained in our case as revealed from Fig. 2 a, b which show that the values of both the effective permittivity and effective permeability are equal through the studied frequencies band. Figure 2c also shows that the real part of the relative impedance is approximately unity through the operating frequency band. Figure 6 shows the calculated absorptivity by the FEM compared to that obtained from Eq. (9) where a good agreement is obtained.

In order to understand the absorption response of the proposed MMA, the absolute of the electric field distributions and surface current are presented in Fig. 7 at two absorption peaks for TE polarized incident wave. Figure 7a, c show the absolute of the electric field and surface current at 16.2 GHz. However, Fig. 7b, d show the absolute of the electric field and surface current at 26.4 GHz. It may be noted from Fig. 7a, b that the electric field

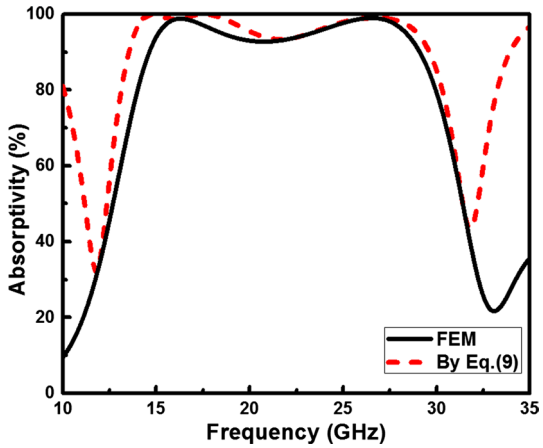

Fig. 6 The calculated absorptivity of the proposed MMA by the FEM via CST softaware (solid black line), and that from Eq. (9) (red dash line)

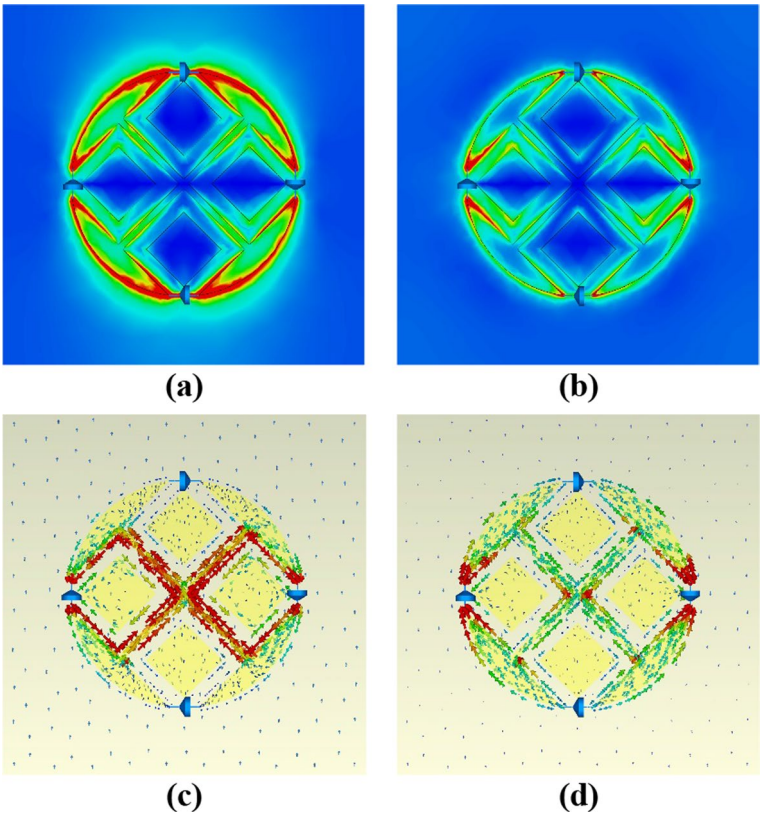

Fig. 7 The simulated electric field distribution at **a** 16.2 GHz and **b** 26.4 GHz, and the simulated surface current distribution at **c** 16.2 GHz, and **d** 26.4 GHz

is concentrated at the fringe of the metallic circle which indicate the presence of electric resonance. Further, Fig. 7c, d reveal that the surface current is concentrated at the metallic cross using supported magnetic resonance. Due to presence of both electric and magnetic resonance responses, a perfect and broadband absorber is obtained.

Figure 8 shows the effect of the incident angle on the absorption response and absorption bandwidth of the reported MMA. This investigation has been done for both TE and TM polarizations. The suggested MMA has a good absorption (above 80%) with the variation of the incident angle (up to 50°). It may be seen that the proposed MMA has an identical response for both TE and TM polarization with variation of the incident angle.

The geometrical parameters are next studied to investigate their effect on both the absorptivity and absorption frequency band of the absorber. Figure 9a shows the impact of substrate thickness on the absorption response. During this study, the geometrical parameters are fixed at their initial values. It may be noted from Fig. 9a that reducing the substrate thickness increases the absorption frequency band while the absorptivity decreases. This is due to the effect of the substrate thickness on the metamaterial impedance and hence the impedance matching. Consequently, the substrate thickness of 1.6 mm is taken as an optimum value. However, Fig. 9b shows the effect of the radius of the metallic circle in the top metallic layer on the MMA performance. It may be seen

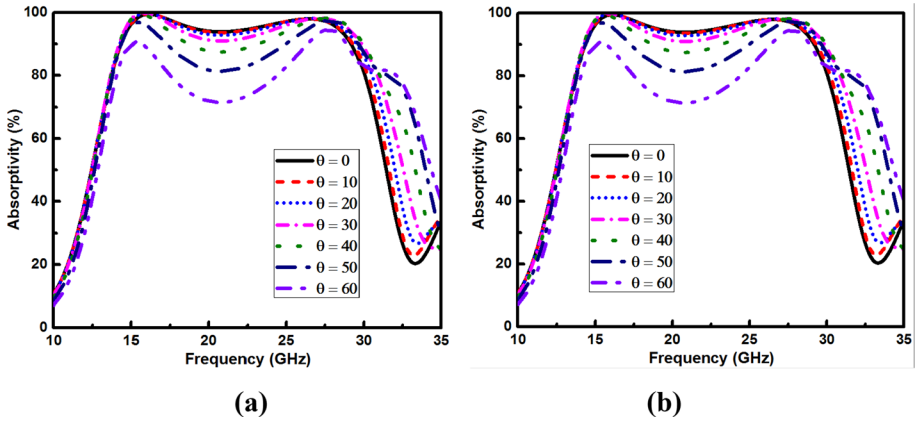

Fig. 8 The impact of the incident angle on the absorptivity for **a** TE and **b** TM polarizations

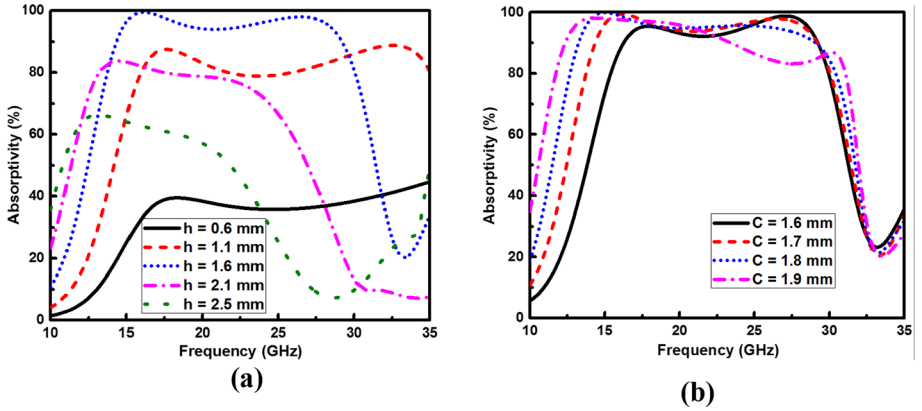

Fig. 9 The effect of **a** the substrate thickness h and **b** the radius of the metallic circle c on the absorption of the proposed absorber

from Fig. 9b that, reducing the radius of the metallic circle leads to narrower absorption frequency band and higher absorptivity. Therefore, the radius of 1.7 mm is the optimum value with high absorption of 99.9% over broadband of frequencies from 14.35 to 29.18 GHz.

Next, the impact of the periodicity of the unit cell is investigated as shown in Fig. 10a. It may be seen from Fig. 10a that by reduces the periodicity of the proposed unit cell, the absorption frequency band is broadens but the absorptivity decreases. So, the optimum value is 5.5 mm as shown in Fig. 10a. The effect of the etched square length on the absorption response is studied. As shown in Fig. 10b, the optimum value is 2.7 mm with high absorption of 99.9%.

Figure 11a shows the effect of the metallic cross width on the absorptivity and the absorption band where an optimum value of 0.1 mm is obtained. However, Fig. 11b shows that an optimum surface mount resistor of 240 Ω with a good absorption response. The optimum values of the geometrical parameters are shown in Table 1.

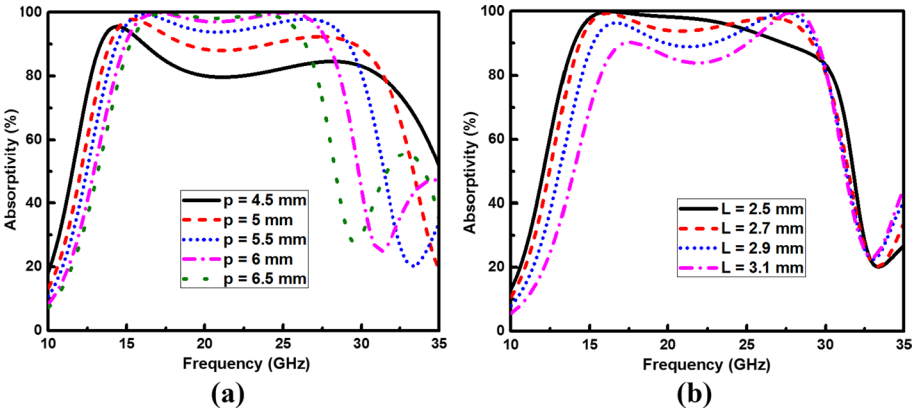

Fig. 10 The effect of **a** the periodicity of unit cell p and **b** the length of the etched square, on the absorption of the proposed metamaterial absorber

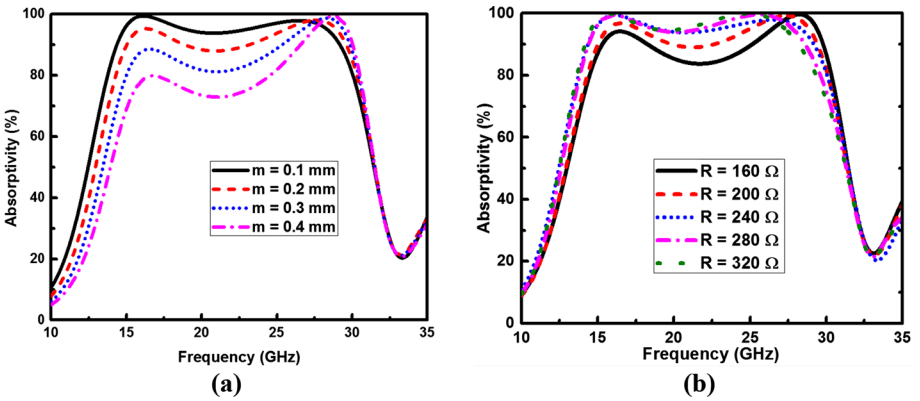

Fig. 11 The effect of **a** the width of the metallic cross m and **b** the value of the surface mount resistor, on the absorption of the proposed metamaterial absorber

Table 1 The optimum geometrical parameters of the reported metamaterial absorber

Parameter	*H*	*c*	*p*	*L*	*m*	*R*
Value (mm)	1.6	1.7	5.5	2.7	0.1	240 Ω

It is worth noting that the variation of the absorptivity and the absorption frequency band with the geometrical parameters can be referred to the impact of each geometrical parameter on metamaterial impedance and hence on the impedance matching. Consequently, the optimum geometrical parameters shown in Table 1 achieve the matching impedance between the metamaterial impedance and the free space impedance.

Table 2 The tolerance of different geometric parameters of the proposed design

Parameter	Tolerance (%)	Maximum absorptivity (%)	Operating frequency band (GHz)
h	+5	97.56	13.7–28.2
	− 5	99.96	14.1–28.8
C	+5	99.886	15.8–30
	− 5	99.97	16.3–30
L	+5	99.23	15.3–30
	− 5	99.985	15.5–29.7
m	+5	98.96	14.2–29
	− 5	99.17	15.2–30

A tolerance study has been also done to ensure that the proposed MMA is robust to the fabrication errors. Table 2 shows the effect of the fabrication errors on the maximum absorptivity and the operating frequency band. In this study, one parameter is tested while the other geometrical parameters are kept constant at their optimum values. It may be seen from this table that the suggested MMA has a tolerance of ± 5% where the maximum absorptivity is still better than 97% and the operating frequency band is still wider than 13.7 GHz.

Table 3 shows a comparison between the proposed broadband MMA relative to the recent reported broadband absorbers. It may be seen that many of recent published articles are based on multi-layered or/and loaded resistors to improve the absorption frequency band. However, other recent published articles are depended on using a resistive film pattern of indium tin oxide (ITO) with/without 3D structure such as Hao et al. (2022), Zolfaghary pour (2023), Ruan et al. (2023), Wang et al. (2020) to expand the operating frequency band. Additionally, Norouzi et al. (2023) improved the absorption frequency band by using 3D structure of graphite based on resistive film. Therefore, the proposed MMA has advantages in terms of ultrathin, broadband, compact size and polarization insensitive compared to those based on the planar structure and conventional metallic layer.

4 Conclusion

In this paper, an ultrathin, broadband, polarization insensitive and perfect metamaterial absorber is proposed and investigated. The structure is based on symmetric resonators using single substrate layer of low cost FR-4 and with four surface mount resistors. The reported MMA has absorptivity above 90% over broadband frequency range from 14.35 to 29.18 GHz for both TE and TM polarizations. Also, the suggested design has a high absorption response (above 80% of absorptivity) with incident angle variation (up to 50°) with a subwavelength unit cell (0.076λ). Due to the advantages of the proposed design such as; compactness, broadband, high absorption and polarization insensitivity with simple design, it can be used for many potential applications including stealth technology, specific absorption rate (SAR) reduction and antennas in reducing sidelobe radiation.

Table 3 A comparison between the proposed broadband MMA relative to the recent reported broadband absorbers

Ref./structure shape	Working frequency (GHz)	Periodicity of unit cell (mm)	Thickness	Maximum Absorptivity (%)	Number of resistors/ layers	Top layer
This work	14.35–29.18	5.5 × 5.5	1.6	99.9	4/Single	Copper
(Nguyen et al. 2021) Defected metallic resonator loaded with four lumped resistors	8–18	9.7 × 9.7	2.5	99.7	4/Single	Copper
(Cheng et al. 2020) four coplanar asymmetric sectional resonator	7.18–8.8	20 × 20	2	98.9	–/Single	Copper
(Suo et al. 2023) Planar ITO resonator	14.3–18.3	10 × 10	1.94	99	4/Five	ITO
(Wang and Cheng 2020) Meander wire structure	1.84–5.96	10 × 10	10	85	4/Single	Copper
(Xiong et al. 2022) Six scalloped ITO at the top layer and square ITO in the middle layer	6.6–18.0	10 × 10	4.525	99	–/Five	ITO
(Hao et al. 2022) Multiple resonators at different layers	8.6–75.8	16 × 16	3.53	> 90	–/Eight	Resistive film pattern of ITO
(Puri and Singh 2022) Resonating patches at the top	13.6–18.5	9 × 9	1.6	> 97	–/–	Copper
(Zolfaghary pour 2023) Array of conductive ribbons	7.1 to 13.8	15	6	> 90	–/–	Conductive polylactic acid
(Norouzi et al. 2023) Eight 45-degree hollow sections made of graphite	35–400	2.5	1.05	> 85	–/–	Graphite + resistive film patch array (3D structure)
(Ma et al. 2022) Two ring resonators	5.5–14.4	20.2	10.3	> 90	8/Five	Copper
(Ruan et al. 2023) ITO pattern etched on PET + PMI + backplane	11.2–42.8	12	2.388	> 90	−/Four	Resistive ink and ITO
(Wang et al. 2022) 3D grid structure and traditional magnetic materials	5–20	8	5.8	> 90	−/Four	3D resistive film structure

Table 3 (continued)

Ref./structure shape	Working frequency (GHz)	Periodicity of unit cell (mm)	Thickness	Maximum Absorptivity (%)	Number of resistors/ layers	Top layer
(Wang et al. 2020) 3D resistive metamaterial	3.7–40	8	7.3	> 90	–/Three	3D resistive with traditional magnetic absorbing material
(Han et al. 2022) Frequency selective surface	9.16–17.8	10	2	99.85	–/Single	Copper

Author contributions ASS has proposed the idea. AMS, AMA, and MOS have done the simulations of the reported absorber. All authors have contributed in the analysis, discussion, writing and revision of the paper.

Funding Open access funding provided by The Science, Technology & Innovation Funding Authority (STDF) in cooperation with The Egyptian Knowledge Bank (EKB). No fund is associated with the current manuscript.

Availability of data and materials The data will be available upon request.

Declarations

Conflict of interest The authors would like to clarify that there is no financial/non-financial interests that are directly or indirectly related to the work submitted for publication.

References

Abouelatta, M.A., Hameed, M.F., Obayya, S.S.: Highly efficient ultrathin broadband quarter-waveplate based on plasmonic metasurface. Optik **239**, 166770 (2021a). https://doi.org/10.1016/j.ijleo.2021.166770

Abouelatta, M.A., Obayya, S.S., Hameed, M.F.: Highly efficient transmissive metasurface for polarization control. Opt. Quant. Electron. **53**(2), 1–1 (2021b). https://doi.org/10.1007/s11082-020-02697-8

Azab, M.Y., Hameed, M.F., Nasr, A.M., Obayya, S.S.: Highly sensitive metamaterial biosensor for cancer early detection. IEEE Sens. J. **21**(6), 7748–7755 (2021). https://doi.org/10.1109/JSEN.2021.3051075

Bağmancı, M., Akgöl, O., Özaktürk, M., Karaaslan, M., Ünal, E., Bakır, M.: Polarization independent broadband metamaterial absorber for microwave applications. Int. J. RF Microw. Comput. Aided Eng. **29**(1), e21630 (2019). https://doi.org/10.1002/mmce.21630

Chen, H., Yang, X., Wu, S., Zhang, D., Xiao, H., Huang, K., Zhu, Z., Yuan, J.: Flexible and conformable broadband metamaterial absorber with wide-angle and polarization stability for radar application. Mater. Res. Express **5**(1), 015804 (2018). https://doi.org/10.1088/2053-1591/aaa7ab

Chen, K., Luo, X., Ding, G., Zhao, J., Feng, Y., Jiang, T.: Broadband microwave metamaterial absorber with lumped resistor loading. EPJ Appl. Metamater. **6**, 1 (2019). https://doi.org/10.1051/epjam/2018011

Chen, H., Huang, Y., Li, G., He, Q., Xie, J., Deng, L.: Design and experimental validation of a low-profile wideband metamaterial absorber by characteristic modes analysis. Results Phys. **28**, 104684 (2021). https://doi.org/10.1016/j.rinp.2021.104684

Cheng, Y., Luo, H., Chen, F.: Broadband metamaterial microwave absorber based on asymmetric sectional resonator structures. J. Appl. Phys. **127**(21), 214902 (2020)

Cheng, Y., Qian, Y., Luo, H., Chen, F., Cheng, Z.: Terahertz narrowband perfect metasurface absorber based on micro-ring-shaped GaAs array for enhanced refractive index sensing. Physica E **1**(146), 115527 (2023)

Cong, L.L., Cao, X.Y., Song, T., Gao, J., Lan, J.X.: Angular-and polarization-insensitive ultrathin double-layered metamaterial absorber for ultra-wideband application. Sci. Rep. **8**(1), 1–2 (2018). https://doi.org/10.1038/s41598-018-28041-5

Du, Z., Liang, J., Cai, T., Wang, G., Deng, T., Wu, B.: Designing an ultra-thin and wideband low-frequency absorber based on lumped resistance. Opt. Express **30**(2), 914–925 (2022). https://doi.org/10.1364/OE.445081

Engheta, N., Ziolkowski, R.W. (eds.): Metamaterials: Physics and Engineering Explorations. Wiley, New York (2006)

Fan, S., Song, Y.: Ultra-wideband flexible absorber in microwave frequency band. Materials **13**(21), 4883 (2020). https://doi.org/10.3390/ma13214883

Fan, Y., Wang, J., Fu, X., Li, Y., Pang, Y., Zheng, L., Yan, M., Zhang, J., Qu, S.: Recent developments of metamaterials/metasurfaces for RCS reduction. EPJ Appl. Metamater. **6**, 15 (2019). https://doi.org/10.1051/epjam/2019008

Ghosh, S., Bhattacharyya, S., Srivastava, K.V.: Design, characterisation and fabrication of a broadband polarisation-insensitive multi-layer circuit analogue absorber. IET Microw. Antennas Propag. **10**(8), 850–855 (2016). https://doi.org/10.1049/iet-map.2015.0653

Hao, J., Zhang, B., Jing, H., Wei, Y., Wang, J., Qu, Z., Duan, J.: A transparent ultra-broadband microwave absorber basedon flexible multilayer structure. Opt. Mater. **1**(128), 112173 (2022). https://doi.org/10.1016/j.optmat.2022.112173

https://www.cst.com/.

Kalraiya, S., Chaudhary, R.K., Abdalla, M.A.: Design and analysis of polarization independent conformal wideband metamaterial absorber using resistor loaded sector shaped resonators. J. Appl. Phys. **125**(13), 134904 (2019). https://doi.org/10.1063/1.5085253

Karaaslan, M., Bağmancı, M., Ünal, E., Akgol, O., Altıntaş, O., Sabah, C.: Broad band metamaterial absorber based on wheel resonators with lumped elements for microwave energy harvesting. Opt. Quant. Electron. **50**(5), 1–8 (2018). https://doi.org/10.1007/s11082-018-1484-2

Landy, N.I., Sajuyigbe, S., Mock, J.J., Smith, D.R., Padilla, W.J.: Perfect metamaterial absorber. Phys. Rev. Lett. **100**(20), 207402 (2008). https://doi.org/10.1103/PhysRevLett.100.207402

Li, H., Yuan, L.H., Zhou, B., Shen, X.P., Cheng, Q., Cui, T.J.: Ultrathin multiband gigahertz metamaterial absorbers. J. Appl. Phys. **110**(1), 014909 (2011). https://doi.org/10.1063/1.3608246

Li, Z., Cheng, Y., Luo, H., Chen, F., Li, X.: Dual-band tunable terahertz perfect absorber based on all-dielectric InSb resonator structure for sensing application. J. Alloys Compd. **5**(925), 166617 (2022)

Nguyen, T.T., Lim, S.: Design of metamaterial absorber using eight-resistive-arm cell for simultaneous broadband and wide-incidence-angle absorption. Sci. Rep. **8**(1), 1 (2018). https://doi.org/10.1038/s41598-018-25074-8

Nguyen, T.K., Cao, T.N., Nguyen, N.H., Bui, X.K., Truong, C.L., Vu, D.L., Nguyen, T.Q.: Simple design of a wideband and wide-angle insensitive metamaterial absorber using lumped resistors for X-and Ku-bands. IEEE Photonics J. **13**(3), 1 (2021). https://doi.org/10.1109/JPHOT.2021.3085320

Norouzi, M., Jarchi, S., Ghaffari-Miab, M., Esfandiari, M., Lalbakhsh, A., Koziel, S., Reisenfeld, S., Moloudian, G.: 3D metamaterial ultra-wideband absorber for curved surface. Sci. Rep. **13**(1), 1043 (2023). https://doi.org/10.1038/s41598-023-28021-4

Puri, V., Singh, H.S.: Design and analysis of a compact ultrathin ultra-wideband metamaterial absorber with near tounity absorption for Ku-band. Int. J. RF Microw. Comput.-Aided Eng. **32**(4), e23069. (2022). https://doi.org/10.1002/mmce.23069

Ruan, J.F., Meng, Z.F., Zou, R.Z., Pan, S.M., Ji, S.W.: Ultra-wideband metamaterial absorber based on frequency selective resistive film for 5G spectrum. Microw. Optical. Technol. L. **65**(1), 20–7 (2023). https://doi.org/10.1002/mop.33441

Saadeldin, A.S., Hameed, M.F., Elkaramany, E.M., Obayya, S.S.: Highly sensitive terahertz metamaterial sensor. IEEE Sens. J. **19**(18), 7993–7999 (2019). https://doi.org/10.1109/JSEN.2019.2918214

Schurig, D., Mock, J.J., Justice, B.J., Cummer, S.A., Pendry, J.B., Starr, A.F., Smith, D.R.: Metamaterial electromagnetic cloak at microwave frequencies. Science **314**(5801), 977–980 (2006). https://doi.org/10.1126/science.1133628

Shen, Q., Xiong, H.: An amplitude and frequency tunable terahertz absorber. Results Phys. **1**(34), 105263 (2022)

Suo, M., Xiong, H., Li, X.K., Liu, Q.F., Zhang, H.Q.: A flexible transparent absorber bandwidth expansion design based on characteristic modes. Results Phys. **6**, 106265 (2023)

Wang, Q., Cheng, Y.: Compact and low-frequency broadband microwave metamaterial absorber based on meander wire structure loaded resistors. AEU Int. J. Electron. Commun. **1**(120), 153198 (2020)

Watts, C.M., Liu, X., Padilla, W.J.: Metamaterial electromagnetic wave absorbers. Adv. Mater. **24**(23), 98–120 (2012). https://doi.org/10.1002/adma.201200674

Xie, S., Zhu, L., Zhang, Y., Ji, Z., Wang, J.: Three-dimensional periodic structured absorber for broadband electromagnetic radiation absorption. Electron. Mater. Lett. **16**, 340–346 (2020)

Xiong, H., Hong, J.S., Luo, C.M., Zhong, L.L.: An ultrathin and broadband metamaterial absorber using multi-layer structures. J. Appl. Phys. **114**(6), 064109 (2013). https://doi.org/10.1063/1.4818318

Xiong, H., Long, T.B., Shi, T., Jiang, B.X., Zhang, J.T.: Wideband and polarization-insensitive metamaterial absorber with loading lumped resistors. Appl. Opt. **59**(23), 7092–7098 (2020). https://doi.org/10.1364/AO.395904

Xiong, Y., Chen, F., Cheng, Y., Luo, H.: Rational design and fabrication of optically transparent broadband microwave absorber with multilayer structure based on indium tin oxide. J. Alloys Compd. **5**(920), 166008 (2022)

Yang, J., Shen, Z.: A thin and broadband absorber using double-square loops. IEEE Antennas Wirel. Propag. Lett. **15**(6), 388–391 (2007). https://doi.org/10.1109/LAWP.2007.903496

Yoo, M., Lim, S.: Polarization-independent and ultrawideband metamaterial absorber using a hexagonal artificial impedance surface and a resistor–capacitor layer. IEEE Trans. Antennas Propag. **62**(5), 2652–2658 (2014). https://doi.org/10.1109/TAP.2014.2308511

Zhang, H., Tian, X., Zhang, H., Zhang, D.: Three-dimensional gravity tailored ultra-broadband absorber based on a high-impedance surface. JOSA B. **38**(3), 866–875 (2021)

Zhu, W.: Electromagnetic metamaterial absorbers: From narrowband to broadband [Internet]. Metamaterials and Metasurfaces. IntechOpen; 2019. Available from: http://dx.doi.org/10.5772/intechopen.78581

Zolfaghary pour, S., Chegini, E., Mighanim M.: Design of wideband metamaterial absorber using circuit theory for X-band applications. IET Microw. Antennas Propag. **17**(4), 292–300 (2023). https://doi.org/10.1049/mia2.12338